

Effect of high energy ball milling on the structure of iron – multiwall carbon nanotubes (MWCNT) composite

Akshay Kumar^a, U. Pandel and M.K. Banerjee*

Department of Metallurgical and Materials Engineering, Malaviya National Institute of Technology, Jaipur, India

(Received April 22, 2017, Revised November 9, 2017, Accepted December 7, 2017)

Abstract. High energy ball milling is employed to produce iron matrix- multiwall carbon nanotube (MWCNT) reinforced composite. The damage caused to MWCNT due to harsh ball milling condition and its influence on interfacial bonding is studied. Different amount of MWCNT is used to find the optimal percentage of MWCNT for avoidance of the formation of chemical reaction product at the matrix - reinforcement interface. Effect of process control agent is assessed by the use of different materials for the purpose. It is observed that ethanol as a process control agent (PCA) causes degradation of MWCNT reinforcements after milling for two hours whereas solid stearic acid used as process control agent, allows satisfactory conservation of MWCNT structure. It is further noted that at a high MWCNT content (~ 2wt.%), high energy ball milling leads to reaction of iron and carbon and forms iron carbide (cementite) at the iron-MWCNT interface. At low percentage of MWCNT, dissolution of carbon in iron takes place and the amount of reinforcement in iron matrix composite becomes negligibly small. However, under the present ball milling condition (ball to metal ratio~ 6:1 and 200 rpm vial speed) iron-1wt.% MWCNT composite of good interfacial bonding can retain the tubular structure of reinforcing MWCNT.

Keywords: Multi Wall Carbon Nanotube (MWCNT); composite; Mechanical Alloying (MA); X-ray diffraction; transmission electron microscopy; interfacial bonding

1. Introduction

Due to attractive physical and mechanical properties, carbon nanotubes have attracted special attention of the researchers to explore its employment in a number of useful applications (Bakshi *et al.* 2010, Iijima 1991, El-sherbiny *et al.* 2013). Nonlinear vibration properties of multiwall carbon nanotubes, its buckling behavior under load and other physical and mechanical behavior of MWCNT have been elegantly studied by previous workers (Rakrak *et al.* 2016, Chemi *et al.* 2015, Kazemi *et al.* 2014). There are reports on the capability of magnetic particle filled CNTs to absorb microwaves (Dillon *et al.* 2012, Vishlaghi and Ataie 2014). Success in the development of CNT reinforced polymer matrix composites has stimulated new researches for development of nanocomposites based on metal matrix. It is known that high aspect ratio along with Vander Waals forces among CNTs make it difficult to disperse CNTs uniformly within a metal matrix. Several fabrication methods are so far tried for production of uniformly distributed Metal- MWCNT nano-

*Corresponding author, Professor, E-mail: mkbanerjee@hotmail.com

^a Ph.D. Student, E-mail: akshay.kumar428@gmail.com

composites (Paul *et al.* 2013). Differential density between metal and CNT makes it difficult to secure to uniform distribution of CNT in metal matrix. Mechanical alloying route is reported to be a successful method of preparing metal matrix – CNT composite. Moreover, It is reported that mechanical alloying route has been successful in fabrication of aluminum- MWCNT composites with reasonably good distribution of reinforcing material (Basariya *et al.* 2014, Peng and Chang 2014, Zhou *et al.* 2016, Maleque *et al.* 2016). It is also reported that molecular level mixing of copper, iron in MWCNT suspension followed by drying, calcinations, reduction and spark plasma sintering can produce nanocomposite with homogenous distribution of CNTs with copper matrix (Cha *et al.* 2005). Poor interfacial bonding and agglomerating tendency of MWCNTs are considered to be responsible for causing problems in securing reproducibility in structure and properties of metal matrix MWCNT reinforced composites. In spite of success in production of metal-MWCNT composite, fabrication of iron matrix-MWCNT composites by high energy ball milling bears the risk of damage at the surface of MWCNT. This is because the solubility of carbon atoms in iron is quite high. Moreover, iron has high affinity for carbon to form its carbide. Hence mechanical alloying can lead to the formation of carbide at the matrix-MWCNT interface through mechano-chemical synthesis of MWCNT and the matrix metal. While some researchers believe this reaction to be a genuine danger in harnessing the potential advantage of MWCNT as reinforcement, there are others who opine that the formation of carbide in aluminum-MWCNT interface reduces the wettability angle and thus aids in achieving a better interfacial bonding (Chen *et al.* 2017, Zhou *et al.* 2016).

Iron – CNT composite bears the potential application in data storage device, sensors and many applications where high strength, high conductivity magnetic materials are needed. Since attempt to produce iron-MWCNT composite through mechanical alloying route is scarce in literature, it seems worthy to study structural evolution in high energy ball milled iron-MWCNT composite containing varying amounts of MWCNT. Attempts are also made to evolve means for conservation of graphite structure of MWCNT.

2. Experimental work

2.1 Materials

The materials used for the present study are the multiwall carbon nanotubes (MWCNT) and iron powders of predetermined sizes and shapes. The purity of iron powder (Sigma Aldrich) is greater than 99% and its size is 325 mesh (~ 44 micron). The iron powders of irregular shape, make up the metal matrix; MWCNTs fabricated by chemical vapor deposition (CVD) technique has the purity 98wt.%; its outer diameter is 1-2 nm and the length is around 3-8 micron. Scanning Electron microscopy and high resolution transmission electron microscopy (HRTEM) are used to examine the morphology of as received iron powder and the MWCNT used in the present study (Fig. 1).

2.2 Method of preparation

High energy ball milling of mixture of iron powder and MWCNT was carried out by the use of both solid and liquid process control agent (stearic acid and ethanol respectively). MWCNT content has been varied from 0.5wt.% to 2wt.%. After sonication of MWCNT in 50 ml of ethanol

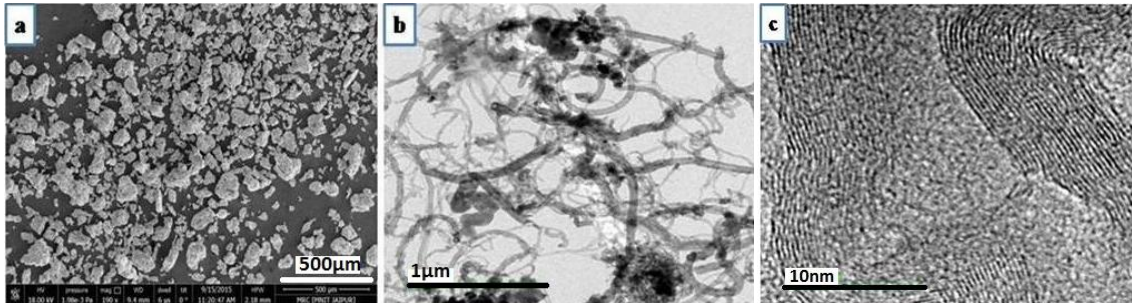


Fig. 1 (a) SEM image of as received pure iron powder; (b) TEM image of as received MWCNT; and (c) HRTEM image of MWCNT showing multiple walls

for 10 minutes, iron powders were added and ultrasonication of the suspension is continued for 5 minutes. Evaporation of ethanol is accomplished by heating the mixture at 50°C for 30 mins. The mixture is then subjected to high energy ball milling (HEBM) for two hours with ball to powder ratio 6:1 (BPR) at a vial speed of 200 rpm. The air inside the vial was flushed out by passing pure Argon gas. The use of argon gas during milling operation is very vital as it controls surface and interface contamination which may occur during the synthesization of the composite mixture via high energy ball milling. Moreover, the employment of minimum milling speed and time has helped in preventing contamination.

However to fully ascertain if there is objectionable contaminating effect due to aerial nitrogen or oxygen within the vial, separate experiments are needed.

Stearic acid is used as process control agent for all compositions of composite. Also, ethanol as liquid process control agent (PCA) has been tried in high energy ball milling of iron-1wt.% MWCNT powder mix with ball to powder ratio of 6:1 at a milling speed of 200 rpm. After a number of trials the ball milling time is fixed at 2 hours; similarly the trials were made to find the minimum quantity of process control agents which could cause least damage to MWCNTs. The ball milling operation was stopped periodically to avoid heat buildup in the milling container and the temperature of powder under milling was always maintained at room temperature. This is done to avoid the chemical degradation of CNT by way which in turn could affect electrical and physical properties of the composite.

2.3 Characterization of ball milled composites

Microstructural study of nanocomposites of different MWCNT content was conducted by field emission scanning electron microscope of model, NOVA NANOSEM 450, at an accelerating voltage of 15KV. X-ray diffraction study was carried with the aid of Xpert-Pro Pan Analytical model XRD system. XRD experiment was conducted within angular range of 20-80° for the powder sample at scan speed of 2°/min. High resolution transmission electron microscope (Tecnai G²20 FEI S Twin) is employed for microstructural study at high resolution. Small quantity of powder sample is dispersed in absolute alcohol and then ultrasonicated for 30 minutes; 20 μl of suspension is withdrawn from the top and is dropped on carbon coated grid. The sample is put to HRTEM observation after complete evaporation of ethanol.

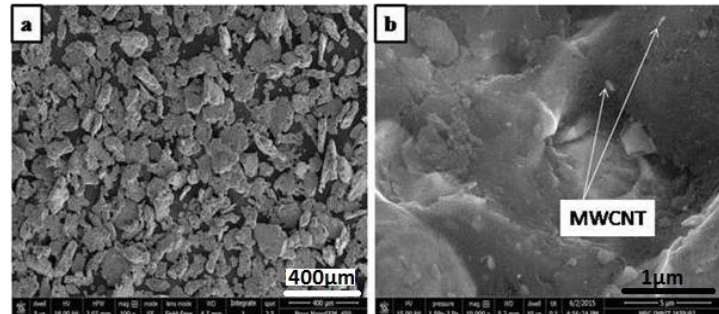


Fig. 2 (a) SEM image of 1wt.% of MWCNT composite, showing flattening of metal particles; and (b) SEM image of the same sample at higher magnification; structure shows that MWCNTs are embedded at places (white arrow)

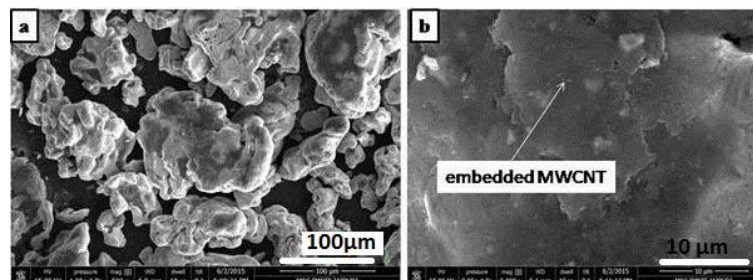


Fig. 3 (a) SEM image of 2wt % of MWCNT in iron matrix showing morphology of powder after 2 hrs milling; and (b) SEM image at higher magnification showing embedded MWCNT

3. Result and discussion

3.1 SEM analysis

The microstructures of HEBM composites are shown in Figs. 2 and 3. Fig. 2 reveals that in Fe-1wt.% MWCNT composite, MWCNT are embedded in the matrix of iron particles which have been flattened due to high energy ball milling for two hours. It is also observed that the MWCNTs have become shorter in length due to ball milling. This observation is in agreement with previous investigations (Choi *et al.* 2009).

In case of composite containing 2wt.% MWCNT, it does not seem that flattening of iron particles has been as good as in 1wt.% MWCNT containing composites (Fig. 3(a)). Increasing the MWCNT content is known to exhibit higher tendency for agglomeration due to Vander Waal's forces of attraction. Also, higher MWCNT content within metal matrix puts more resistance to deformation of metal particles because of the fact that a higher amount of MWCNT in the composite would share higher amount of energy imposed onto the system during high energy ball milling. At the same time, high population density of MWCNT restricts the radial flow of metallic materials and so metal particles have become constrained in flattening at higher concentration of MWCNTs (2wt.%). Moreover, the microstructures in Figs. 2(b) and 3(b) show that the interfacial bonding is apparently good after 2-hour ball milling.

3.2 XRD analysis

X-ray diffraction study is conducted to monitor the evolution of structural constituents in iron-MWCNT composites. Fig. 4 shows the XRD spectra of composites containing different quantity of MWCNT reinforcement. It can be seen in the spectrum of Fe-0.5wt.% MWCNT that no characteristic peak of MWCNT is present in the said XRD spectrum. However in case of both the 1wt.% MWCNT and 2wt.% MWCNT containing iron matrix composites, prominent peaks of cementite can be observed in the corresponding XRD spectrum in Fig. 4. The prominent peak observed at 26.4° in the XRD spectrum of Fe-1wt.% MWCNT composite is indexed as CNT (002). It is thus ascertained that MWCNT as reinforcing constituent retains its structural identity in HEBM iron-1wt.% composite. However, upon increase in the amount of MWCNT to 2wt.%, the characteristic XRD peak of MWCNT is absent in the concerned XRD spectrum. Instead only characteristic peak of cementite (Fe_3C) is recorded in the above spectrum. The absence of any MWCNT peak in XRD spectrum of HEBM iron - MWCNT powder mix may be due to two reasons: (1) HEBM induced damage of graphitic structure of MWCNT has led to dissolution of carbon in the lattice of iron; and/or (2) mechano-chemical activation has led to synthesis of iron, and carbon to give rise to the formation of iron carbide viz. cementite with orthorhombic crystal structure. When amount of MWCNT is small ($\sim 0.5\text{wt.}\%$), only dissolution of carbon can take place and there may not be any CNT peak in corresponding diffractogram. Moreover, cementite cannot form under this situation. It may be mentioned that the equilibrium solubility of carbon in iron is only $0.025\text{wt.}\%$ at 723°C and naturally this poses a question of how it is possible that there is no peak of CNT and at the same time any peak due to carbide is also absent. This can be explained only if it is surmised that ferrite so formed due to HEBM of iron - MWCNT mixture has remained supersaturated. Supersaturation of ferrite with carbon is feasible under non-equilibrium situation as it prevails during high energy ball milling. However, the supersaturated solid solution is prone to cause precipitation of carbide under normal circumstances. The absence of carbide peak in the XRD spectrum of Fe-0.5wt.% MWCNT composite suggests that the carbon atoms are segregated at the dislocations which are produced aplenty within the iron crystals due to harsh ball milling condition. Such type of super saturation is reported in heavily cold deformed high carbon steels (Languillaum *et al.* 1997). It may be mentioned that ball milling of iron – MWCNT mixture has led to the formation of minor amount of iron oxide. The absence of iron oxide peak in XRD spectrum of Fe-0.5wt.% MWCNT is spurious and is ascribed to low relative counts secured in the XRD experiment which has masked the low intensity oxide peak. Fig. 5 demonstrates that the (110) peak of bcc iron in Fe-1wt.% MWCNT undergoes a shift towards low angle side after two hours of high energy ball milling. Such shift of peak towards lower angle side implies that there has been an increase in lattice parameter; such increase in lattice parameter stems from dissolution of carbon in iron. However, when the MWCNT content is increased to 2wt.%, the XRD spectrum shows peaks of cementite (Fe_3C) instead of MWCNT peaks. This suggests that all the MWCNTs are now consumed by HEBM induced chemical reaction between iron and carbon. It is thus seen that at quite low MWCNT content, dissolution of carbon in iron results in the absence of MWCNT peak in the concerned XRD spectrum, whereas at significantly higher MWCNT content, formation of iron carbide appears to be the main reason of absence of reinforcement peaks in the X-ray diffractogram.

In contrast with XRD results for iron-1wt.% MWCNT composite ball milled with solid stearic acid as PCA, the XRD spectrum of similar Fe-1wt.% MWCNT prepared by the same HEBM procedure but with the use of ethanol as PCA does not show any CNT peak in the XRD spectrum.

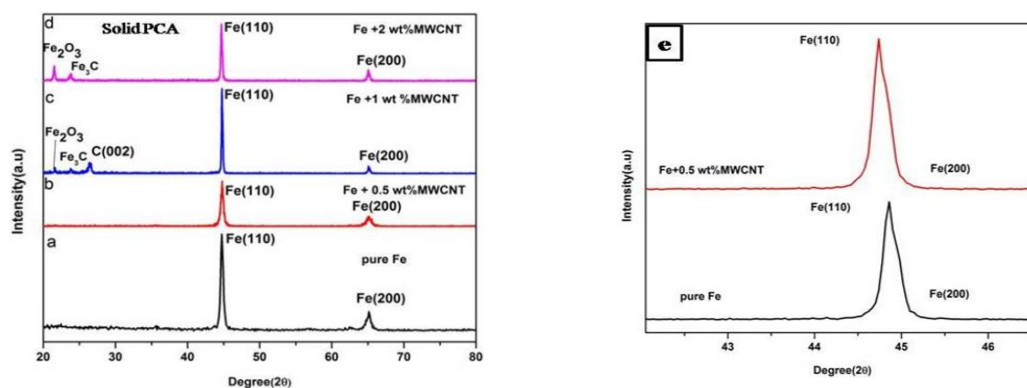


Fig. 4 XRD spectra of the (a) pure iron; (b) Fe+ 0.5wt% MWCNT; (c) Fe+1wt% MWCNT; and (d) Fe+2wt% MWCNT composite after 2 hours HEBM; and (e) Shifting of (110) Fe peak to lower angle in case of Fe+0.5wt% MWCNT

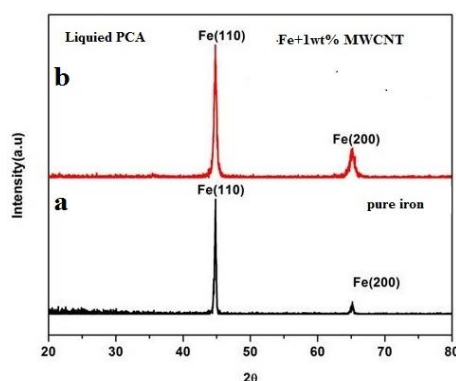


Fig. 5 XRD spectra of (a) pure iron; and (b) Fe+1wt.%MWCNT composite after 2 hrs HEBM by wet method; no CNT peak is observed

Absence of any carbide peak in case of Fe-1wt.% MWCNT composite produced with solid stearic acid as PCA, rules out the possibility of occurrence of any interfacial chemical between iron and carbon. On the contrary, the absence of either peak in case of use of ethanol as the PCA verifies that chemical degradation of MWCNT has taken place due to reaction between ethanol and MWCNT exposed to 50°C. It is therefore conjectured that the conservation of tubular structure of MWCNT is realized in case of 1wt.% MWCNT composites if HEBM is carried out for two hours with solid PCA, viz. stearic acid.

3.3 Transmission electron microscopy

The high-resolution transmission electron microscopic observation indicates that interfacial bonding attainable in Fe-MWCNT composite is quite good. The delineation of a smooth interface between Fe and MWCNT in high energy ball milled composite containing 1wt.% MWCNT corroborates the results of X-ray diffraction. HRTEM photographs of iron-1wt.% MWCNT is presented in Fig. 6 High resolution image records the presence of both MWCNT and pure iron.

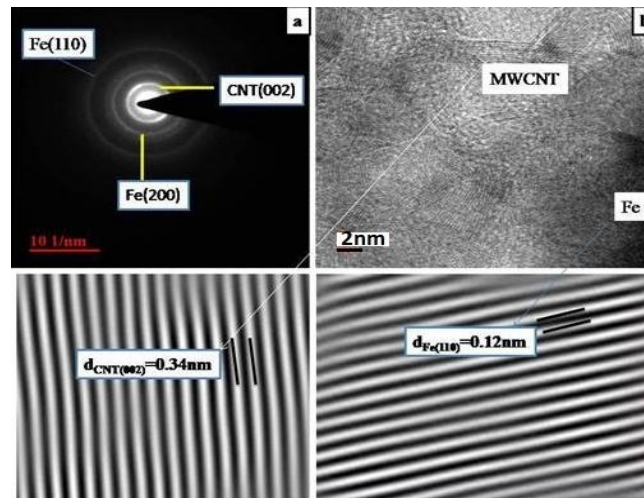


Fig. 6 (a) shows the SAED pattern of Fe+1wt.% MWCNT composite; (b) HRTEM image of Fe+1wt.% MWCNT composite and corresponding lattice images show the d spacing of CNT and Ferrite

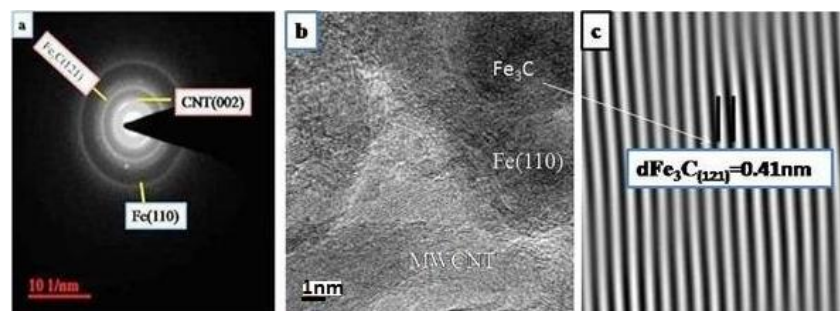


Fig. 7 (a) shows the SAED pattern of Fe+2wt.% MWCNT composite; (b) HRTEM image of Fe+2wt.% MWCNT composite shows Fe (110), CNT (002) and cementite (112) phase; and (c) shows the corresponding d spacing of cementite (Fe_3C)

The interplanar spacing, 0.34 nm of MWCNT characterizes (002) CNT and verifies that graphite structure of MWCNT is conserved. The corresponding SAED pattern presents continuous ring pattern of MWCNT. The evidence of ring pattern from (110) Fe implies that crystals of iron are very fine. In case of Fe-2wt.% MWCNT composite, the high-resolution image reveals the presence of cementite particles (Fig. 7). The formation of cementite in high energy ball milled Fe-2wt.% MWCNT composite has also been recorded in the corresponding XRD spectrum and is thought to be due to mechano-chemical activation during two hours HEBM of Fe-MWCNT composite containing as high as 2wt.% MWCNT. Besides (002) CNT rings, the SAED pattern of Fe-2wt.% MWCNT also exhibits ring pattern of iron due to its fine crystal size. The diffused ring pattern of iron as seen in Fig. 7 is suggestive of the fact that iron crystals are considerably strained. This strain originates from high amount of ball milling energy partitioned into iron particles. This increases the dislocation density in iron crystals. It is known that these dislocations can act as sites for segregation of carbon atoms (Languillaum *et al.* 1997). Due to close proximity between iron and carbon atoms, 2p-3d hybridization occur (Munir *et al.* 2015) and a very good interfacial

bonding is ensured. Thus, it is found that at low concentration of MWCNT, carbon dissolves in iron during HEBM and intense ball milling at high MWCNT content (~2wt.%) leads to carbide formation. However, at 1wt.% MWCNT level, cementite is not found to form.

3.4 Raman spectroscopy

The Raman Spectra of pristine MWCNT and Fe-MWCNT composites are furnished in Fig. 7. It is apparent that pristine MWCNT records characteristic *G* (graphite) and *D* (defect) band at 1350 and 1552 cm^{-1} . The strong *G* and *D* peaks authenticate perfect graphite structure of MWCNTs. Another peak observed at 2700 cm^{-1} has been assigned as *G'* band by previous workers (Poirier *et al.* 2009, Suh and Bae 2013). While the change in size and shape of *G* and *D* bands (viz. widening and shortening) suggests introduction of defects in the graphite structure of MWCNT, the degradation in MWCNT structure is also associated with shift of position of *G* and *D* bands in Raman Spectra. Moreover, the ratio of intensities of *D* and *G* band, i.e., I_D/I_G gives the idea of the magnitude of damage, if any, in MWCNT structure. Raman Spectroscopic results of HEBM composites are furnished in summarized form in Table 1.

It can be seen from Table 1, that I_D/I_G ratio of composite samples, high energy ball milled for two hours, increases with increase in MWCNT content; also, a shift of *G* band towards higher wave number may be noticed. These observations have the implication that MWCNT milled with iron has undergone considerable structural damage. Degradation of MWCNT structure under severe ball milling has also been reported in the literature (Choi *et al.* 2012). Structural damage of reinforcing MWCNT is also substantiated by the change in size and shape *D* and *G* band in the present experiments. From the appearance of peaks of *G* and *D* band in ball milled composite samples it seems that complete amorphization of MWCNT has not taken place in the present experimental condition. The *G'* band is seen to have been flattened due to ball milling and this hints upon significant damage of MWCNT in 2wt.% composite after HEBM for 2 hours. Such damage of MWCNT may disrupt its C-C bonds and can make carbon atoms available for segregation at dislocations within iron crystals. This helps in 3d-2p hybridization between iron and MWCNT; hence a very good interfacial bonding is obtained. However severe damage of MWCNT in composite of high reinforcement content (~2wt.% MWCNT) leads to higher concentration of carbon atoms segregating at the dislocations. This may ultimately lead to supersaturation of iron with carbon and hence may promote precipitation of cementite within iron crystal as observed in HRTEM (Fig. 7). Formation of cementite due to direct mechano-chemical synthesis of iron and carbon is equally probable. Such chemical reaction between iron and carbon gives rise to the formation of cementite which is distinctly evidenced in the Raman spectrum of Fe-2wt.% MWCNT composite (Fig. 8).

The Raman spectroscopy is used to observe shape size and position of *G* and *D* bands so that structural integrity of CNT can be assessed. In this study, we found that there are prominent bands for 2wt.% MWCNT but their size, shape and position have been altered considerably. At the same time *G'* band for this composite is widened and considerably flattened in 2%MWCNT composite along with structural damage of CNT due to ball milling. This implies that some amorphisation of MWCNT has taken place. We do not see the CNT peak in XRD in line with above observation of Raman Spectroscopy. However, in the XRD patterns we cannot see amorphous graphite due to the reason that overall degree of amorphisation is not so high as to be detected by XRD. Moreover, the carbon atoms have undergone mechano-chemical synthesis with iron and have formed carbides. So, cementite peak is seen with diminution in intensity of CNT (graphitic structure) in the concerned

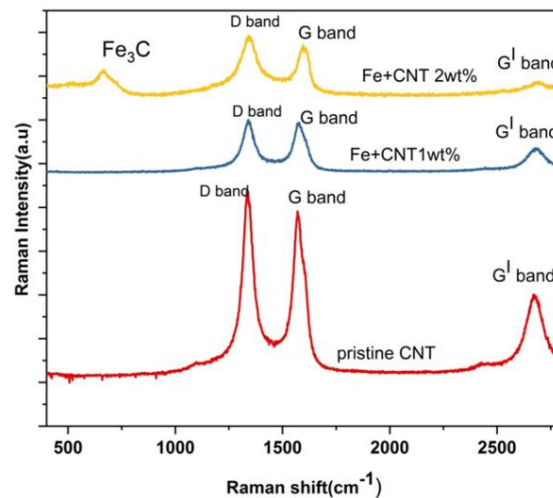


Fig. 8 Raman spectra of pristine MWCNT and of Fe-MWCNT nanocomposites containing different weight percent of MWCNT

Table 1 Summarized results of Raman Spectroscopy

Sample	Raman peak shift (Cm ⁻¹)		I_D/I_G
	D band	G band	
Pristine MWCNT	1343	1571	.98
Fe+1wt.% MWCNT 2 hrs milling	1349	1575	1.02

Table 2 Properties of experimental composites

Sample name	Magnetic saturation Ms (emu/gms)	Remanent magnetisation (Mr) (emu/gms)	Coercivity (Hc) (Oe)	Vickers hardness (Hv)	Compressive strength [mpa]	D.C Electric conductivity σ (Scm ⁻¹)
Fe+1wt%MWCNT	192	0.47	7.23	115	595	1.11×10^5 Scm ⁻¹
Fe+2wt%MWCNT	197	0.49	8.12	125	879	1.85×10^5 Scm ⁻¹

XRD spectrum. Thus formation of cementite, dissolution of carbon in ferrite and partial amorphisation of MWCNT has been responsible for absence of evidence for graphitic structure.

3.5 Properties of iron-MWCNT composites

The mechanical and physical properties of the experimental composites are shown in Table 2. It is observed that there has been considerable improvement in strength and hardness values owing to composite hardening. The MWCNT has also led to significant rise in electrical conductivity at high saturation magnetization. The unique properties of CNTs are responsible for this type of improvement. However detailed study is required for proper understanding of causative factors responsible for such improvement in properties.

4. Conclusions

The authors conclude that high energy ball milling with tailored process parameters can be used effectively to produce iron-MWCNT composite. Severe ball milling at high MWCNT content leads to chemical degradation of MWCNT. Mechano-chemical activation leads to the formation of iron carbide at the interface. A very good interfacial bonding is achievable after ball milling of iron-1wt.% MWCNT composite for two hours.

References

- Bakshi, S.K., Lahiri, D. and Agarwal, A. (2010), "Carbon nanotube reinforced metal matrix composites – A review", *Int. Mater. Rev.*, **55**(1), 41-64.
- Basariya, M.R., Srivastava, V.C. and Mukhopadhyay, N.K. (2014), "Microstructural characteristics and mechanical properties of carbon nanotube reinforced aluminum alloy composites produced by ball milling", *Mater. Des.*, **64**, 542-549.
- Cha, S.I., Kim, K.T., Arshad, S.N., Mo, C.B. and Hong, S.H. (2005), "Extraordinary strengthening effect of carbon nanotubes in metal-matrix nanocomposites processed by molecular-level mixing", *Adv. Mater.*, **17**(11), 1377-1381. DOI: 10.1002/adma.200401933
- Chemi, A., Heireche, H., Zidour, M., Rakrak, K. and Bousahla, A.A. (2015), "Critical buckling load of chiral double-walled carbon nanotube using non-local theory elasticity", *Adv. Nano Res., Int. J.*, **3**(4), 193-206.
- Chen, B., Shen, J., Ye, X., Imai, H., Umeda, J., Takahashi, M. and Kondoh, K. (2017), "Solid-state interfacial reaction and load transfer efficiency in carbon nanotubes (CNTs)-reinforced aluminum matrix composites", *Carbon*, **114**, 198-208.
- Choi, H., Shin, J., Min, B., Park, J. and Bae, D. (2009), "Reinforcing effects of carbon nanotubes in structural aluminum matrix nanocomposites", *J. Mater. Res.*, **24**(8), 2610-2616.
- Choi, H.J., Shin, J.H. and Bae, D.H. (2012), "The effect of milling conditions on microstructures and mechanical properties of Al/MWCNT composites", *Composites Part A*, **43**(7), 1061-1072.
- Dillon, F.C., Bajpai, A., Koo, S.A., Downes, S., Aslam, Z. and Grobert, N. (2012), "Tuning the magnetic properties of iron-filled carbon nanotubes", *Carbon*, **50**(10), 3674-3681.
- El-sherbiny, Sh.G., Wageh, S., Elhalafawy, S.M. and Sharsha, A.A. (2013), "Carbon nanotube antennas analysis and applications: review", *Adv. Nano Res., Int. J.*, **1**(1), 13-27.
- Iijima, S. (1991), "Helical microtubules of graphitic carbon", *Nature*, **354**(6348), 56-58.
- Kazemi, M.H., Akhavan-Behabadi, M.A. and Nasr, M. (2014), "Convective heat transfer of MWCNT / HT-B Oil nanofluid inside micro-fin helical tubes under uniform wall temperature condition", *Adv. Nano Res., Int. J.*, **2**(2), 99-109.
- Languillaume, J., Kapelski, G. and Baudelet, B. (1997), "Cementite dissolution in heavily cold drawn pearlitic steel wires", *Acta Mater.*, **45**(3), 1201-1212.
- Maleque, M.A., Abdullah, U., Yaacob, I. and Ali, Y. (2016), "Characterization of ball-milled carbon nanotube dispersed aluminum mixed powders", *IOP Conf. Ser.: Mater. Sci. Eng.*, **123**(1), 1-6.
- Munir, K.S., Qian, M., Li, Y., Oldfield, D.T., Kingshott, P., Zhu, D.M. and Wen, C. (2015), "Quantitative analysis of MWCNT-Ti powder mixtures using Raman spectroscopy: The influence of milling parameters on nonstructural evolution", *Adv. Eng. Mater.*, **17**(11), 1660-1669.
- Paul, R., Kumbhakar, P. and Mitra, A.K. (2013), "A facile chemical synthesis of a novel photo catalyst: SWCNT/titania nanocomposite", *Adv. Nano Res., Int. J.*, **1**(2), 71-82.
- Peng, T. and Chang, I. (2014), "Mechanical alloying of multi-walled carbon nanotubes reinforced aluminum composite powder", *Powder Technology*, **266**, 7-15.
- Poirier, D., Gauvin, R. and Drew, R.A.L. (2009), "Structural characterization of a mechanically milled carbon nanotube/aluminum mixture", *Compos. A*, **40**(9), 1482-1489.

- Rakrak, K., Zidour, M., Heireche, H., Bousahla, A.A. and Chemi, A. (2016), "Free vibration analysis of chiral double-walled carbon nanotube using non-local elasticity theory", *Adv. Nano Res., Int. J.*, **4**(1), 31-44.
- Suh, J.Y. and Bae, D.H. (2013), "Mechanical properties of Fe-based composites reinforced with multi-walled carbon nanotubes", *Mater. Sci. Eng. A*, **582**, 321-325.
- Vishlaghi, M.B. and Ataie, A. (2014), "Investigation on solid solubility and physical properties of Cu-Fe/CNT nano-composite prepared via mechanical alloying route", *Powder Technology*, **268**, 102-109.
- Zhou, W.W., Bang, S., Kurita, H., Miyazaki, T., Fan, Y. and Kawasaki, A. (2016), "Interface and interfacial reactions in multi-walled carbon nanotube reinforced aluminum matrix composites", *Carbon*, **96**, 919-928.
- Zhou, W., Bang, S., Kurita, H., Miyazaki, T., Fan, Y. and Kawasaki, A. (2017), "Interface and interfacial reactions in multi-walled carbon nanotube reinforced aluminum matrix composite", *Carbon*, **96**, 919-928.

CC